# Rapid and Precise Method for Analysis of Energy Dispersive X-Ray Spectra

A new, precise, and rapid method for the analysis of energy dispersive x-ray spectra generated by electron beam or x-ray excitation is presented. It includes the use of Gaussian profiles and a polynomial of 1/E (where E is the x-ray energy) to represent the observed x-ray characteristic lines and background, automatic sectioning of the entire spectrum, and a figure of merit to estimate goodness of fit. Details of the method and its programming techniques are given. Results of analyzing complicated energy dispersive x-ray (EDX) spectra of multi-element alloys are presented.

## Introduction

There has been a growing interest in the use of solid state detectors for x-ray spectroscopy by the energy dispersive method (EDX) in recent years. However, there are a number of drawbacks in the method which must be overcome if the data are to be used for precise and rapid quantitative analysis. Overlapping spectra from different elements due to relatively poor energy resolution of the detector and the limitation of the input counting rate of the system result in poor counting statistics for the intensities of low-concentration elements.

A number of methods have been reported to solve these problems with various degrees of success. One of the two major approaches is in the use of computer-stored spectra of pure elements to least-squares fit the experimental data. There are a number of disadvantages in this method: the need for collecting and storing numerous standard spectra of pure elements obtained with different experimental conditions, the difficulties in accounting for the change of linewidths, peak shifts due to different experimental conditions or specimens, and the statistical counting errors in the stored standard spectra. The other approach is the fitting of observed data to calculated profiles by using Gaussian curves to represent x-ray emission lines [1]. Because the observed spectra closely match Gaussian profiles, the fitted Gaussians are free of statistical errors, and the overlap problems can be handled very well by this approach, it is considered to be a better method [2].

The approach used in this report is the same as our previous method [1a, 2] with the new additions of automatic sectioning of the entire spectrum to reduce unnecessary calculations, the use of well-established x-ray data to determine the number of characteristic lines present, and the introduction of a figure of merit to estimate the quality of the results for each element. Compared to our previous method, the present program is approximately five times or more faster, and has the same precision.

# Basic mathematical models for the profile-fitting method

It is essential for quantitative analysis of EDX by the profile-fitting method (PFM) to determine the functions that best represent the x-ray emission lines, the background contributions and the effect of the solid state detector on the observed data. By knowing the shapes of x-ray lines and their background, plus the response of the detector, high precision results can be obtained by PFM, including the case of relatively poor statistical experimental data. Brief descriptions of the mathematical models used in this method are given in the following sections.

## **Detector efficiency correction**

In general, three effects must be corrected for in the observed intensities collected by a solid state detector. These include the absorptions of the beryllium window and the thin gold contact surface, and the transparency of the silicon or germanium crystal. The observed intensity

Copyright 1979 by International Business Machines Corporation. Copying is permitted without payment of royalty provided that (1) each reproduction is done without alteration and (2) the *Journal* reference and IBM copyright notice are included on the first page. The title and abstract may be used without further permission in computer-based and other information-service systems. Permission to *republish* other excerpts should be obtained from the Editor.

can be expressed as

$$I_{\text{observed}}(E) = DEF(E) I_{\text{incident}}(E),$$
 (1)

and

$$DEF(E) = \exp \left[ -(\mu t)_{Be} \right] \exp \left[ -(\mu t)_{Au} \right]$$

$$\times \left\{ 1 - \exp \left[ -(\mu t)_{si} \right] \right\}, \tag{2}$$

where DEF represents the detector efficiency. Figure 1 shows the silicon detector efficiency as a function of x-ray energy (E) by using Eqs. (1) and (2). The loss of sensitivity at low energies is due to the absorption of the Be window. For example, the window absorbs more than 30 percent of the incident x-rays with energies of 2 keV or less. The drop in efficiency above 18 keV is dominated by the inability to fully absorb high energy x-rays due to the finite thickness of the active region of the silicon crystal. All these factors will affect the observed data and distort their line profiles, especially those in the low and high energy regions, and should be corrected for in quantitative EDX analysis. The detector has approximately 100 percent efficiency in the energy range between 4 and 18 keV, and this energy region should be used whenever conditions allow.

#### **Background subtraction**

It was found that the second-order polynomial of  $(E_0 - E)/E$  [Eq. (3)] gives a close fit to the x-ray background,  $I_{\rm BG}$ , or bremsstrahlung. This analytical expression was determined from experimental data of a pure Be foil 50  $\mu$ m thick in which no characteristic line or absorption edge occurred and the observed spectrum was only the bremsstrahlung [1a, 3]. Equation (3) has also been successfully fitted to the experimental data of a number of thick foils of Fe, Ni, Ag, and Ta. A more general expression is given in Eq. (4),

$$I_{BG}(E) = A_0 \frac{E_0 - E}{E} + B_0 \left(\frac{E_0 - E}{E}\right)^2$$
 (3)

$$=A_1 + \frac{B_1}{E} + \frac{C_1}{E^2} + \frac{D_1}{E^3},\tag{4}$$

where  $E_0$  is the accelerating voltage for the electrons;  $A_0$  and  $B_0$  are constants that depend on the atomic number, the concentration of each element, and the thickness of the specimen;  $A_1$ ,  $B_1$ ,  $C_1$ , and  $D_1$  are constants that are related to  $A_0$ ,  $B_0$ , and  $E_0$  in the following fashion:  $A_1 = B_0 - A_0$ ,  $B_1 = A_0 E_0 - 2B_0 E_0$ ,  $C_1 = B_0 E_0^2$ , and  $D_1 = 0$ .

Equation (4) is used in this program to represent the experimental background where parameters  $A_1$ ,  $B_1$ ,  $C_1$ , and  $D_1$  are determined by a least-squares fit to the experimental data in regions away from the emission lines and absorption edges. The term  $D_1/E^3$  is added to account for

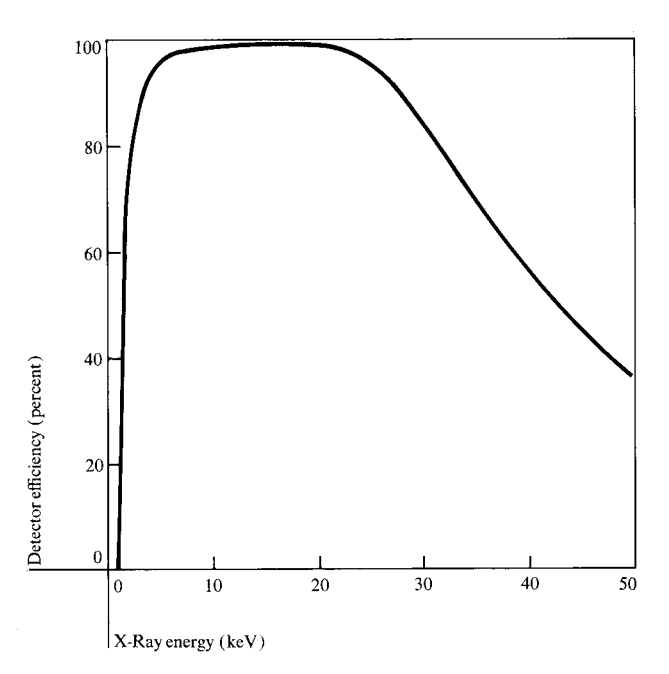
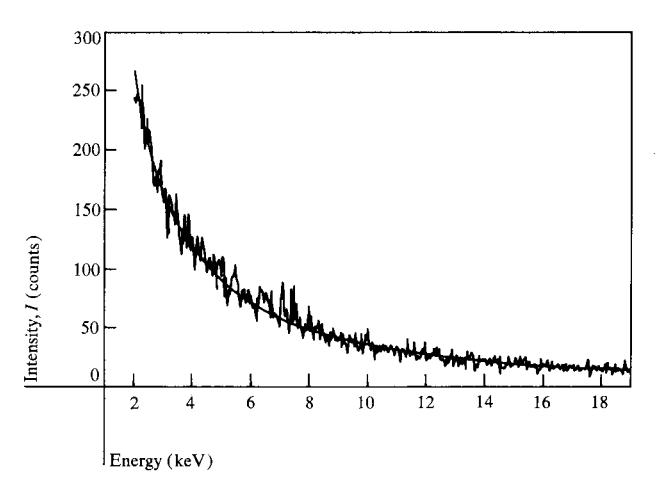


Figure 1 Calculated silicon detector efficiency as a function of x-ray energy, with a 0.025-mm Be window, a  $10^{-3}$ -mm gold contact layer, and a 5-mm Si detector.



**Figure 2** Energy dispersive x-ray (EDX) data for a 50- $\mu$ m Be film were fitted by the background function of  $A_1 + B_1/E + C_1/E^2 + D_1/E^3$ . The excitation voltage was 80 kV.

the probable deviations of the background function from Eq. (3) due to possible errors in the input values for the thicknesses t of Be, Si, and Au, or the electronic circuit. The result of the fitting of Eq. (4) to the experimental data of a Be thin film is shown in Fig. 2. Even though Eq. (4) was originally derived for bremsstrahlung generated by electron-beam excitation, it applies to x-ray excitation cases as well. A slightly different expression of Eq. (3) was also used by Lifshin [4]. In fact, the method of using polynomials to represent a slowly varying function is a very common mathematical practice.

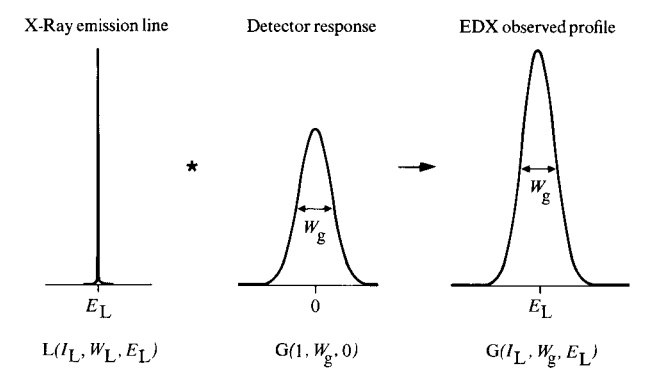
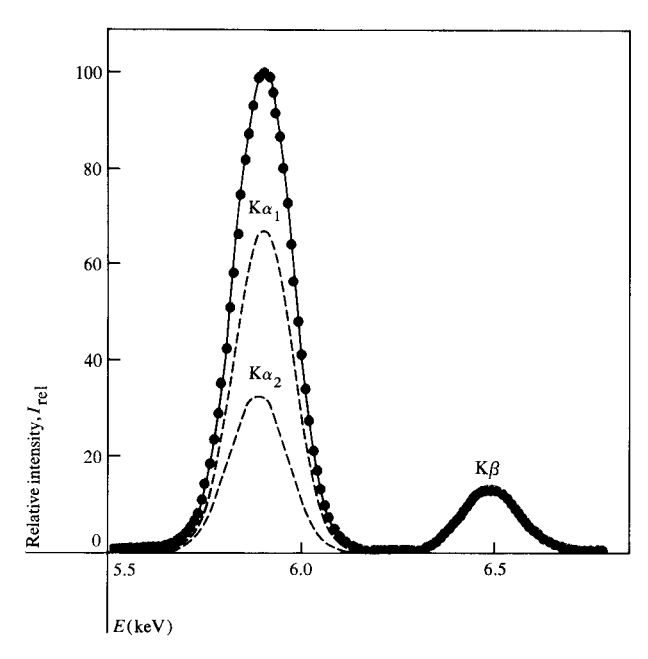


Figure 3 The convolution of a narrow x-ray emission line and a broad Gaussian-type detector response results in a broad Gaussian-like observed profile. (\*) denotes convolution and  $W_g$  is the linewidth of the Gaussian curve.



**Figure 4** The EDX data of the Mn K spectra (solid dots) are fitted by three Gaussians, one each for the  $K\alpha_1$ ,  $K\alpha_2$ , and  $K\beta$  lines (dashed lines). The sum of these three Gaussians (solid line) matches the EDX data.

# Energy dispersive x-ray (EDX) line profiles

It is well known that the x-ray emission lines are Lorentzian with linewidths at half maximum of a few eV [5]. On the other hand, the energy responses of the solid state detector are broad Gaussians [4] and are about 50 times (or more) wider than the x-ray emission lines. As demonstrated in Fig. 3, due to the much broader nature of the Gaussian response of the detector, the x-ray Lorentzian line can be approximated as a delta function. As a result of the convolution of these two functions, the observed EDX line profile is completely dominated by the

detector function and can be closely represented by a Gaussian as shown in Fig. 4 for the Mn  $K\alpha_{1,2}$  and  $K\beta$  lines.

# General description of the programming method

By using the mathematical models described above, a precise and rapid technique for analyzing EDX spectra has been developed. An outline of the programming scheme is given in Fig. 5, and the main features of each major step are described in the following sections. Complicated spectra of super-alloys of Ti, Cr, Mn, Fe, Co, Cu, and W prepared in our laboratory were used to demonstrate the capability of the method.

#### Input

General information about the specimen, including the number of elements present, their symbols, and x-ray lines to be used in analysis, (i.e., K or L lines), are first read into the computer. The program will then read the corresponding line energies and intensity ratios of the principal lines and absorption edges from a pre-stored table. The line energies and intensity ratios in this table are those of Johnson and White [6] with minor modifications. All x-ray lines with intensities greater than one percent of the corresponding principal line have been included, i.e.,  $K\alpha_1$ ,  $K\alpha_2$ ,  $K\beta_1$ ,  $K\beta_2$ ,  $K\beta_3$  for the K series, and  $L\alpha_1$ ,  $L\alpha_2$ ,  $L\beta_1$ ,  $L\beta_2$ ,  $L\beta_3$ ,  $L\beta_4$ ,  $L\gamma_1$ ,  $L\gamma_2$ ,  $L_\ell$ , and  $L_\eta$  for the L series; no line in the M series is used. The lines needed for the analysis are then determined.

# Data processing

The observed EDX data are first corrected for the detector efficiency. This correction is a function of energy that depends on the physical dimensions of the detector, i.e., the thicknesses of the Be window, the silicon (or Ge) crystal, and the gold contact layer. Note that different detectors might have different thicknesses, and the best available values should be used.

After correcting for the detector efficiency, the backgrounds are determined. In an entire EDX spectrum, there are a number of regions that are free of characteristic x-ray lines and contain only background. Data falling in these regions were used to determine the background by fitting with Eq. (4). The upper or lower energy limit for this calculation is set at 4.5 times the half width higher or lower than the x-ray line of maximum or minimum energy for all the elements present. For example, these limits were 9.27 and 4.14 keV for a Ti, Cr, Mn, Fe, Co, Cu, and W super-alloy as shown in Fig. 5. Within this limit, the energy ranges that contain no characteristic line are determined. The criterion for setting these boundaries is that the estimated intensities from all the emission lines in the specimen must be less than the standard deviation of

the background. Figure 6 gives the results of automatic sectioning and the fitted backgrounds.

After the backgrounds have been subtracted, the entire spectrum is divided into a number of sections for profile fitting. The boundary of each section is set at the energy at which its intensity is no more than one standard deviation of the estimated line intensity at that energy. In each section there will be at least one principal line, either  $K\alpha$ , (if  $K\alpha_1$  is in one of the absorption edge regions,  $K\beta_1$  will be used) or  $L\alpha_1$ , of the elements present in the specimen. The regions near the absorption edge of all elements are also determined so that data in these regions will be excluded in the profile fitting. The widths of these regions depend on the energy of the absorption edges and on the intensity of the principal line of the element. In general, the energy range of these regions is approximately equal to the resolution of the detector. Figure 7 shows the fitted sections and the absorption-edge-excluded regions determined by the program for a super-alloy of Ti, Cr, Mn, Fe, Co, Cu, and W.

In fitting the calculated data to the observed data, the calculated x-ray profiles have the following form:

$$I(E) = \sum_{i=1}^{N} P(i) \left\{ \sum_{j=1}^{L_i} R(i,j) \exp \frac{-C[E - E(i,j)]^2}{W^2(i,j)} \right\}, \quad (5)$$

where N is the number of elements in the section;  $L_i$ , the number of lines for element i in the section; P(i), the peak intensity of the principal line  $(K\alpha_1, K\beta_1, \text{ or } L\alpha_1 \text{ of element } i)$ ; R(i, j), the intensity ratio of line j to its principal line for element i; E(i, j), the energy of line j of element i, assumed to be related to E(1, 1) by the expression

$$E(i, j) = E(1, 1) + [P(N + 2)][E_0(i, j) - E_0(1, 1)],$$
 (6)

where  $E_0(i, j)$  is the energy of the j line in element i read from the pre-stored table, P(N + 1) = E(1, 1), C = 0.693, and W(i, j) is the half width of the Gaussian profile on line j of element i, where it is assumed that

$$W^{2}(i,j) = P(N+3)^{2} + P(N+4)[E_{0}(i,j) - E_{0}(1,1)].$$
 (7)

See the Appendix for detailed mathematical derivations.

First N and  $L_i$  are determined and then the I(E) are calculated by profile fitting. In determining I(E), there are N+4 variables  $[P(i), i=1, \cdots, N+4]$  for N elements in the specimen; P(1) to P(N) represent the peak intensities for the principal line of each element; P(N+1) is the energy of the principal line for the first line of the first element; P(N+2) is used to compensate for possible error in the separation between  $E_0(i, j)$  and  $E_0(1, 1)$  and should be very close to 1.0; P(N+3) represents the half width of E(1, 1), namely W(1, 1); and P(N+4) is the parameter used to relate W(i, j) to W(1, 1).

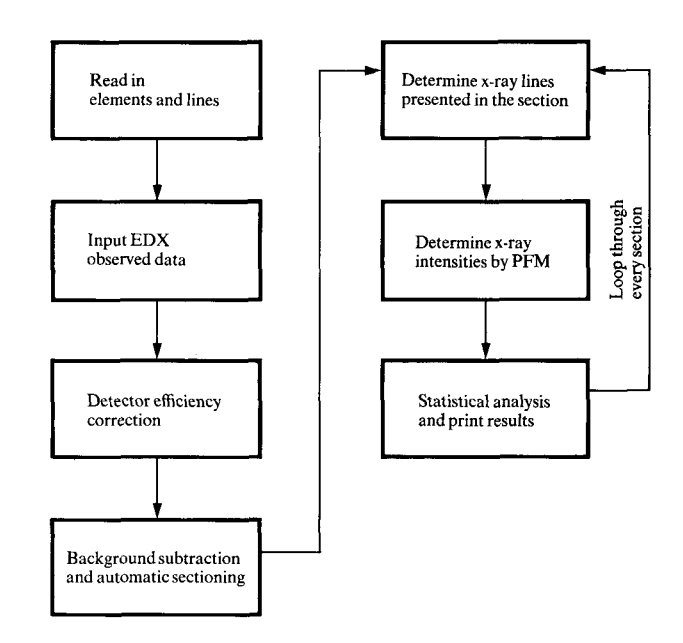


Figure 5 Block diagram of the general programming scheme.

The solution of the profile fitting is obtained by computer search of these N+4 parameters so that the sum-of-squares difference between the calculated and observed data reaches a minimum. The mathematical method used to search for this minimum involves the nonlinear-simplex method of Nelder and Mead [7] with modifications by the author. Robaux's algorithm [8] was used to avoid being trapped in a false minimum. Since our introduction of the application of the simplex method to EDX spectral analysis [1a], the method has generated a lot of interest. For example, it has recently been adapted to EDX analysis by scientists from the National Bureau of Standards [9].

#### Output

The output of the profile fitting method results includes the name of the specimen, the experimental time, the elements present, the x-ray lines used for the calculation, the line energies, the peak intensities, the figures of merit, the estimated precision of peak intensities, and the chisquares of the fit. Peak intensities are the highest intensities of the cluster of  $\alpha$  or  $\beta$  lines. The advantage of using peak intensity instead of integrated intensity is that peak intensity is far less sensitive than the integrated intensity to uncertainties in the background. Precision of the peak intensity is defined as  $\Delta/\delta = (I_{\rm cal} - I_{\rm obs})/\sqrt{I_{\rm obs}}$  at the peak location. In general, it will be less than 2.0. Chisquare is a measure of the match between the calculated and observed profiles. A value of 2.0 or less is considered

209

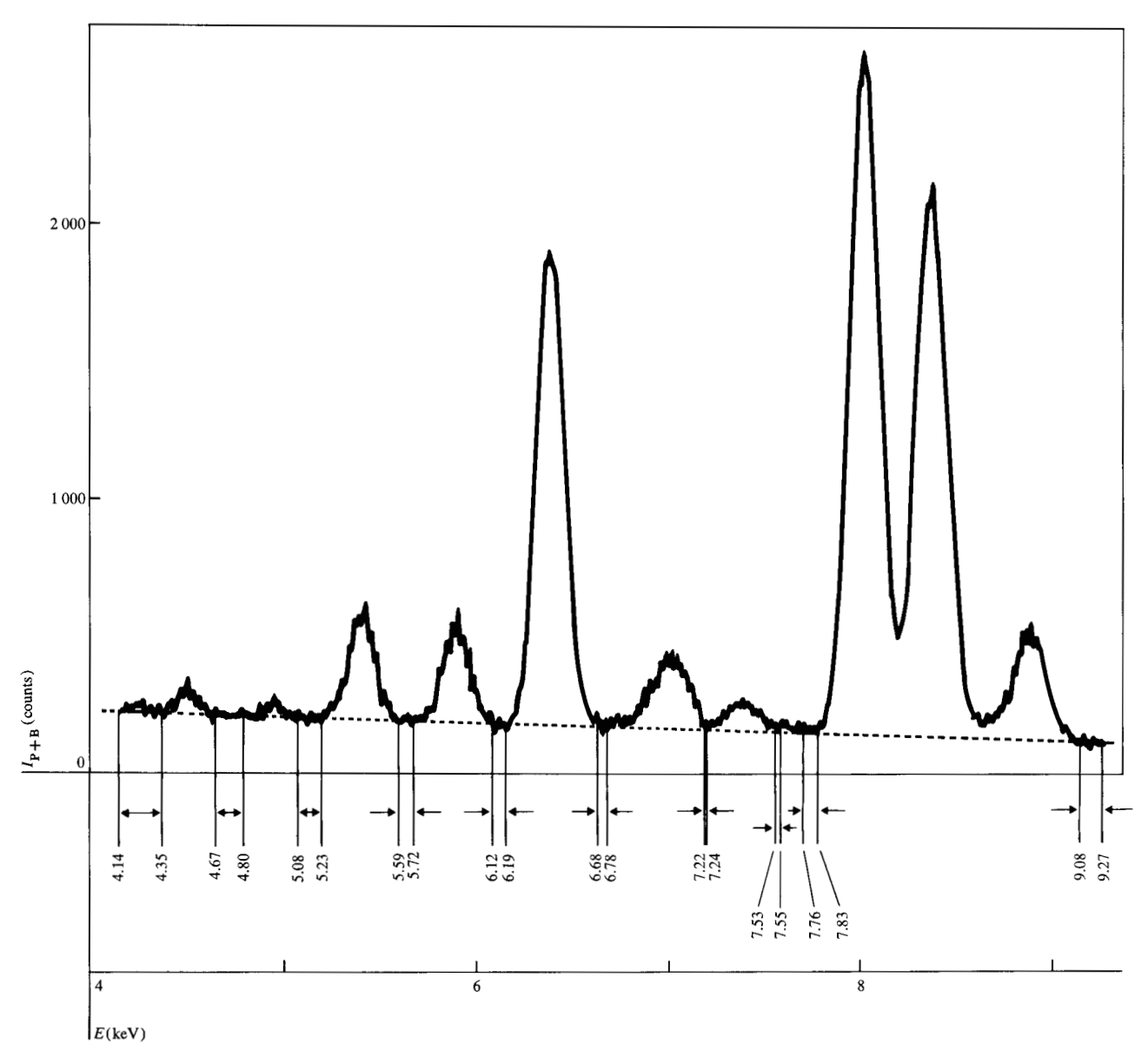


Figure 6 Result of fitting the background function, Eq. (4), to the EDX spectrum of a seven-element (Ti, Cr, Mn, Fe, Co, Cu, and W) specimen, namely, super-alloy 3. Energy ranges of the background-fitted regions are specifically indicated.

acceptable. A figure of merit has been defined for evaluation of the goodness of fit:

Figure of merit = 
$$\frac{1}{\text{Precision}} + \frac{1}{\text{Chi-square}}$$
. (8)

Our experience indicates that a value of 2.0 or more yields good results, values between 2.0 and 1.0 represent fair results, and values less than 1.0 represent poor results. Cases that fall into the poor category are generally due to high values of chi-square; probable causes are the existence of another element or poor experimental data. A rerun of the experiment is required in these cases.

### Results and discussion

Results of using this technique to analyze four complex EDX spectra from separate specimens of super-alloys are given in Table 1. Of these four specimens, the first three contained the same seven elements, Cu, Fe, Cr, Mn, Ti, Co, and W. The last specimen was different, with elements of Mn, Fe, Cu, and W. There are a number of serious overlaps in the first three specimens, e.g., Cr K $\beta$ /Mn K $\alpha$ , Mn K $\beta$ /Co K $\alpha$ . Some elements had very weak intensities which were buried under strong peaks of the adjacent element. These are very good examples for demonstrating the capability of the method.

210

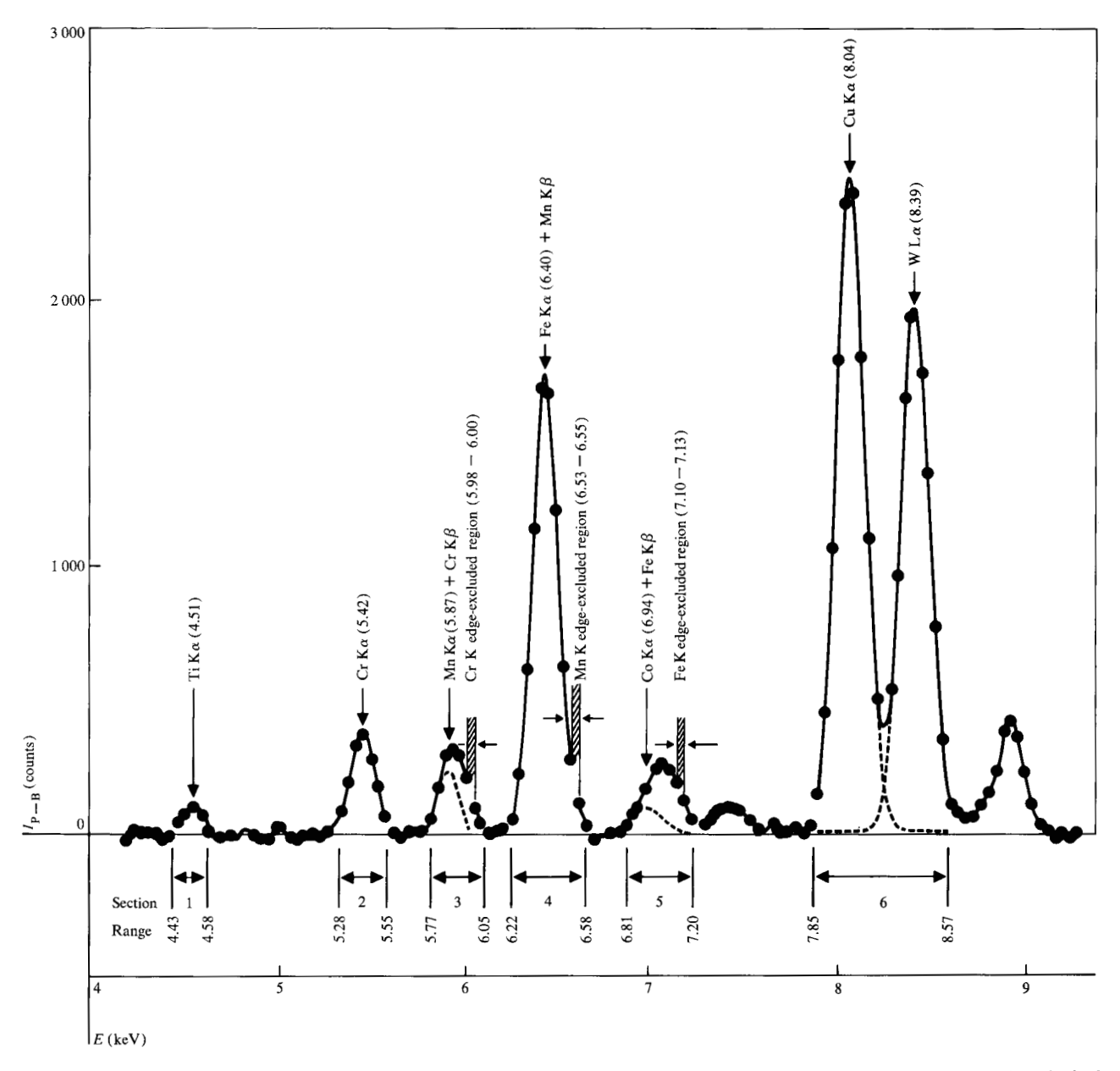


Figure 7 Results of fitting Gaussian profiles, Eq. (5), to the EDX data with background subtracted. The dotted curves are the principal lines in each section and some of these curves coincide with the solid curves, i.e., the total fitted profiles. These solid curves go through all the solid dots (the EDX data are shown for every fourth data point). The boundaries of each section and the absorption-edge-excluded regions are also given.

The total CPU time for the analysis of these four complicated specimens is about 25 seconds, which corresponds to about 1 second per element being analyzed. The results in Table 1 are listed in order of increasing energy of the principal lines used for the elements. Over 90 percent of all the elements being analyzed had figures of merit of better than 2.0; only three lines had values between 2.0 and 1.0, indicating good overall results. Notice the dynamic capability of the method for handling spectra with large variations in peak-to-background ratios in

these specimens. The highest ratio is 27 from W L $\alpha$  and the lowest is only about 0.1 from Co K $\alpha$ , both in superalloy 1. Estimated precisions of the fitted peak intensities were generally less than 1.0, which means that the deviations of the calculated peak intensities from the observed peak intensities are within the statistical accuracy, i.e., within one standard deviation of the peak intensity. Similar results were obtained for the chi-square values; only two lines had values slightly over two. The results of the fitting are also shown in Fig. 6.

Table 1 Listing of computer output (200-second experimental time for all samples).

Sample	Element	Line	keV	Counts	Figure of merit	Precision	Chi-square
Super-alloy 1							
• •	Ti	$K\alpha$	4.51	93.	5.9	0.2	1.2
	Cr	Κα	5.41	893.	2.2	0.9	0.9
	Mn	$K\alpha$	5.89	243.	4.2	0.3	0.8
	Fe	$K\alpha$	6.40	629.	6.0	0.2	0.8
	Co	$K\alpha$	6.89	18.	2.7	0.7	0.8
	Cu	$\mathbf{K}\alpha$	8.04	4738.	3.3	0.4	2.2
	W	$L\alpha$	8.39	5669.	6.9	0.2	2.2
Super-alloy 2							
•	Ti	$K\alpha$	4.52	80.	3.8	0.3	1.2
	Cr	Κα	5.42	290.	1.5	2.0	1.0
	Mn	$K\alpha$	5.89	735.	5.9	0.2	0.7
	Fe	$K\alpha$	6.40	4696.	6.3	0.2	1.4
	Co	$K\alpha$	6.93	337.	9.1	0.1	1.0
	Cu	$K\alpha$	8.04	2092.	11.1	0.1	1.0
	W	$L\alpha$	8.39	1394.	1.7	1.5	1.0
Super-alloy 3							
<b>F</b> = <b>-</b>	Ti	$K\alpha$	4.51	77.	2.3	0.6	1.3
	Cr	$K\alpha$	5.42	389.	3.3	0.4	1.0
	Mn	$K\alpha$	5.87	244.	9.9	0.1	1.3
	Fe	$K\alpha$	6.40	1695.	2.4	0.7	1.0
	Co	$K\alpha$	6.94	96.	2.5	0.8	0.8
	Cu	$K\alpha$	8.04	2453.	3.1	0.4	1.2
	W	$L\alpha$	8.39	1970.	3.0	0.5	1.2
Mn-Fe-Cu-W alloy							
	Mn	$\mathbf{K}\alpha$	5.90	47.	2.4	1.0	0.7
	Fe	Kα	6.40	276.	3.9	0.4	0.8
	Cu	Kα	8.04	696.	1.8	1.8	0.8
	W	Lα	8.37	23.	4.0	0.3	0.9

# Summary

This paper presents a new method for the analysis of EDX spectra. The method includes accurate background subtraction, precision peak intensity determination of all elements present, and corrections of detector efficiency as a function of energy. The precision of the results was estimated in three different ways: the figure of merit, the estimated precision of the peak intensity determination, and the chi-square of the profile fitting. Results for four complicated specimens of super-alloys showed the method to be precise, automatic, rapid, and simple to use.

The conversion of the calculated peak intensities obtained by this method to element concentrations in the specimen can be made by the use of published computer programs or methods. For the electron-beam excitation method, the MAGIC IV program by Colby [10] can be used to analyze bulk specimens, while the analytical schemes proposed by Philibert [11], Kyser [12], and Murata et al. [13] can be used to analyze thin films. In the case of non-dispersive x-ray fluorescence analysis, the LAMA program [14, 15] developed in our laboratory can be used for the analysis of either thin films or bulk specimens.

In general, the choice between using the K or L series x-ray lines in any particular analysis should be determined by the series with energy located in the higher detector efficiency region.

The total length of the present version of the program for this method is about 80K; therefore, in general, it can be run on any moderately sized computer. If only a minicomputer is available, this program must be modified to fit the computer.

The spectral effects of the Si escape peaks are usually less than one percent of the parent lines, and are omitted in this method since the precision and accuracy of x-ray elemental analysis is usually no better than one percent.

#### Acknowledgments

The author thanks R. Geiss for useful discussions and for making the EDX experimental data available, and G. L. Ayers, who designed and built the computer interface to permit rapid transfer of EDX data to the host computer for profile fitting.

# Appendix: Linewidth of the Gaussian response of an EDX system

The full width at half maximum (FWHM) of the observed Gaussian profiles of an EDX system consists of the effective resolution of the detector system and the effects of electronic noise [1b]:

$$FWHM(E)^2 = FWHM(\text{noise})^2 + 2.35^2 F \epsilon E.$$
 (A1)

The second term in Eq. (A1) represents the resolution of the detector system in which F is the Fano factor,  $\epsilon$  is the average energy for electron-hole pair generation; FWHM (noise) is independent of E and assumed to be constant,  $C_1$ , within the same experiment. Equation (A1) can be rewritten as

$$FWHM(E_1)^2 = C_1 + 2.35^2 F \epsilon E_1,$$
 (A2)

and

$$FWHM(E_2)^2 - FWHM(E_1)^2 = 2.35^2 F \epsilon (E_2 - E_1).$$
 (A3)

In terms of half width at half maximum (W), Eq. (A3) becomes

$$W(E_2)^2 - W(E_1)^2 = \frac{2.35^2 F_{\epsilon}}{4} (E_2 - E_1)$$
  
= Constant ×  $(E_2 - E_1)$ 

and

$$W(E_2)^2 = W(E_1)^2 + \text{Constant} \times (E_2 - E_1).$$
 (A4)

By replacing  $E_2$  with  $E_0(i, j)$  and  $E_1$  with  $E_0(1, 1)$ , Eq. (A4) becomes

$$W^{2}(i, j) = W^{2}(1, 1) + \text{Constant}$$
  
  $\times [E_{0}(i, j) - E_{0}(1, 1)].$  (A5)

Let W(1, 1) be represented by the variable P(N + 3), and the constant by P(N + 4). Equation (A5) will lead to the expression

$$W^{2}(i, j) = P(N + 3)^{2} + P(N + 4)$$

$$\times [E_{o}(i, j) - E_{o}(1, 1)]. \tag{7}$$

The above equation gives the relation between W(i, j) and W(1, 1), i.e., P(N + 3). For each section, once these

two variables, P(N + 3) and P(N + 4), are determined by PFM, W(i, j) can then be calculated by Eq. (7).

#### References

- (a) R. H. Geiss and T. C. Huang, "Analytical Transmission Electron Microscopy of Thin Films," J. Vac. Sci. Technol. 12, 140 (1975).
  - (b) R. Fitzgerald and P. Gantzel, "X-Ray Energy Spectrometry in the 0.1 to 10 Å Range," ASTM Special Technical Publication #485 (1971), p. 3.
  - (c) E. Lifshin, "Solid State X-Ray Detectors for Electron Microprobe," ASTM Special Technical Publication #485 (1971), p. 140.
- J. C. Russ, "Processing of Energy-dispersive X-Ray Spectra," X-Ray Spectrom. 6, 47 (1977).
   R. H. Geiss and T. C. Huang, "Quantitative X-Ray Energy
- 3. R. H. Geiss and T. C. Huang, "Quantitative X-Ray Energy Dispersive Analysis with the Transmission Electron Microscope," X-Ray Spectrom. 4, 196 (1975).
- E. Lifshin, "Quantitative Microprobe Analysis with Energy Dispersive Detectors," Adv. X-Ray Anal. 19, 113 (1976).
- A. Hoyt, "The Shape of an X-Ray Line," Phys. Rev. 40, 477 (1932).
- G. G. Johnson and E. W. White, "X-Ray Emission Wavelengths and keV Tables for Nondiffraction Analysis," ASTM Data Series #DS 46 (1970).
- 7. J. A. Nelder and R. Mead, "A Simplex Method for Function Minimization," *Computer J.* 7, 308 (1965).
- 8. O. Robaux, "Analyse des Problèmes de Deconvolution," Rev. du Cethedec NS74-2, 65 (1974).
- 9. C. E. Fiori and D. E. Newbury, "Artifacts Observed in Energy Dispersive X-Ray Spectrometry in Scanning Electron Microscopy," *Proceedings of the 1978 Scanning Electron Microscopy Symposium* 1, 401 (1978).
- 10. J. W. Colby, "Quantitative Microprobe Analysis of Thin Insulating Films," Adv. X-Ray Anal. 11, 287 (1968).
- J. Philibert and R. Trixier, "Electron Probe Microanalysis of TEM Specimens," Electron Microscopy and Microbeam Analysis, Wiley-Interscience Publishers, New York, 1975, p. 333.
- 12. D. Kyser and K. Murata, "Quantitative Electron Microprobe Analysis of Thin Films on Substrates," *IBM J. Res. Develop.* 18, 352 (1974).
- 13. K. Murata, T. Sato, and K. Nagami, "A Simple Quantitative Electron Microprobe Analysis of Multi-element Thin Films on Substrates," *Jpn. J. Appl. Phys.* 15, 2253 (1976).
- D. Laguitton and W. Parrish, "Simultaneous Determination of Composition and Mass Thickness of Thin Films by Quantitative X-Ray Fluorescence Analysis," Anal. Chem. 49, 1152 (1977).
- D. Laguitton and M. Mantler, "LAMA I—A General Fortran Program for Quantitative X-Ray Fluorescence Analysis," Adv. X-Ray Anal. 20, 515 (1977).

Received March 20, 1978; revised September 20, 1978

The author is located at the IBM Research Division laboratory, 5600 Cottle Road, San Jose, California 95193.